Numerical Solutions to Optimal Power-Flow-Constrained Vibratory Energy Harvesting Problems

I. L. Cassidy, W. Song, and J. T. Scruggs

Abstract— **This study addresses the formulation of optimal numerical controllers for stochastically-excited vibratory energy harvesters in which a single-directional power electronic converter is used to regulate power-flow. Single-directional converters have implementation advantages for small-scale applications, but restrict the domain of feasible controllers. Optimizing the average power generated in such systems can be accomplished by formulating the constrained control problem in terms of stochastic Hamilton-Jacobi theory. However, solving the stochastic Hamilton-Jacobi equation (HJE) is challenging because it is a nonlinear partial differential equation. As such, we investigate the capability of the pseudospectral (PS) method to solve the HJE with mixed state-control constraints. The performance of the PS controller is computed for a single-degree-of-freedom resonant oscillator with electromagnetic coupling. We compare the PS performance to the performance of the optimal static admittance controller as well as the optimal unconstrained linear-quadratic-Gaussian controller.**

Index Terms— **Energy harvesting, optimal control, constrained control systems, stochastic systems.**

I. Introduction

The last decade has witnessed the emergence of many technologies that scavenge ambient vibratory energy from their surroundings. The great majority of these developments have been driven by the need to deliver power to small, inaccessible electronic systems, such as embedded wireless sensors, biological implants, and mobile computing applications [1]–[4]. As these systems have evolved, the rate of increase in power and energy demands has been much more rapid than corresponding increases in power and energy densities for localized storage devices, such as batteries [5]. Particular attention has focused on technologies built around piezoelectric and electromagnetic vibratory transduction. High-performance, small-scale energy harvesting poses significant mechanical engineering challenges for efficient design (both in terms of efficient conversion, as well as in terms of space-efficiency). There are electrical engineering challenges as well, to develop efficient power electronic converters operating at the sub-milliwatt scale.

Until recently, most energy harvesting technologies have presumed the available energy to be concentrated in a narrow frequency band, and have made use of classical impedance matching techniques to optimally regulate power generation [6]. However, more recently, attention has begun to shift to broadband energy harvesting problems, in which disturbance energy is stochastic, with wide power spectrum. In this case, the average power generation can be optimized using concepts from stochastic control theory [7], [8]. In particular, Scruggs showed in [8] that if the harvester model is linear and passive, and if the transmission losses in the electronics are resistive (i.e., i^2R losses), then the stochastic energy harvesting problem is equivalent to a sign-indefinite linear-quadratic-Gaussian (LQG) problem. These results have been extended to determine optimal linear feedback controllers for energy harvesters with more complicated transmission loss models, which more realistically capture non-quadratic nature of the parasitic losses in small-scale electronics [9]. However, these extensions have optimized harvested energy only over the domain of linear feedback laws.

This paper constitutes an effort to estimate the maximum-available average power, given a non-quadratic loss model, and with minimal restrictions on the mathematical structure of the feedback law. As such, it allows us to determine the extent to which nonlinear feedback can be used to better compensate for the parasitics in realistic power electronics, as compared to the best linear feedback law. To do this, we frame vibration energy harvesting in the context of stochastic dynamic programming, thus requiring the solution to an associated Hamilton-Jacobi equation (HJE).

As is well known, determining a solution to the HJE is nontrivial, as it requires solution to a partial differential equation over the reachable domain of the state space, and closed-form analytic solutions to the HJE only exist in very specific cases (e.g., LQG and LEQG problems). However, for small-dimensional systems (i.e., 3 or 4 states) it is possible to obtain a numerical solution to the HJE using time stepping schemes coupled with spatial discretizations. For example, finite element [10] and finite volume [11] methods have been effectively applied to solve the HJE, but these methods require significant computational power, making them impractical for problems with multiple dimensions.

Pseudospectral (PS) methods have recently been proposed [12]–[14] to overcome the numerical challenges associated with finite element and finite volume methods and can efficiently solve partial differential equations. The PS method relies on a discretization scheme in which collocation points are chosen based on accurate quadrature rules whose basis functions are typically Chebyshev or Lagrange polynomials. Unlike finite element and finite volume methods, the polynomials used in the PS method are defined over the entire

This work was supported by NSF award CMMI-0747563.

Ian Cassidy is with the Department of Civil and Environmental Engineering, Duke University, Durham, NC 27708, e-mail: ian.cassidy@duke.edu.

Wei Song is with the Department of Civil, Construction, and Environmental Engineering, University of Alabama, Tuscaloosa, AL 35487, e-mail: wsong@eng.ua.edu.

Jeff Scruggs is with the Department of Civil and Environmental Engineering, University of Michigan, Ann Arbor, MI 48109, e-mail: jscruggs@umich.edu.

spatial domain, instead of over subdomains or elements. Furthermore, it has been shown that the PS method can achieve similar accuracy with fewer grid points and less computational memory, as compared to finite element and finite difference methods [12].

Recently, several researchers have applied the PS method to solve a wide range of optimal control problems [15]–[20]. The studies by Elnagar *et al.* [15], [16] are the some of the first to use a PS discretization scheme to solve these types of problems. Those studies obtained the optimal controller for the minimum time problem with nonlinear dynamics using the PS method and compared the optimal controller to other numerical solutions. A subsequent study by Fahroo and Ross [17] applied the PS method to infinite-horizon optimal control problems (e.g., the linear-quadratic-regulator problem). For stochastic systems, the studies by Song and Dyke [19], [20] propose a PS method combined with a successive approximation algorithm to obtain the discretized control manifold. The algorithm proposed in those studies is shown to converge to the optimal solution for a wide range of classical nonlinear dynamical systems.

In this paper, we extend the results presented in [19] and [20] to the stochastic energy harvesting problem. The goal of the energy harvesting problem is to maximize a non-quadratic cost function, which includes a combination of resistive and diode losses in the power electronics used to regulate power-flow. In addition, we include a mixed state-control constraint that results in an instantaneously dissipative controller. Such constraints arise in systems that are controlled using single-directional DC/DC converters, which only permit power to flow from the transducer to storage (but not the other way). Determining numerical controllers for systems with mixed state-control constraints was also investigated by Gong *et al.* [18]. However, the constraints used in that study were saturation limits on the states and controls.

II. The SDOF Stochastic Energy Harvesting Problem with Power-Flow Constraints

Consider the single-degree-of-freedom (SDOF) resonant oscillator with electromagnetic coupling in Fig. 1. As shown, the SDOF oscillator has mass m, damping c, and stiffness k, and the electromagnetic transducer has back-emf motor constant K_t. If we define $x(t)$ as the relative displacement

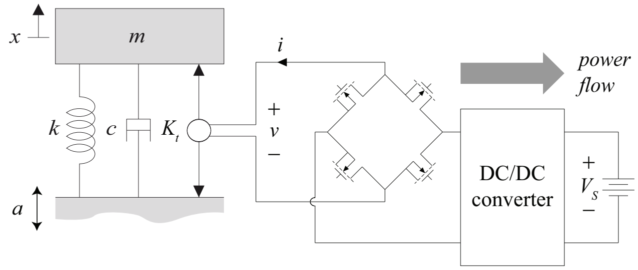

Fig. 1. Electromagnetic energy harvester interfaced with an active bridge rectifier, DC/DC converter, and energy storage.

between the ground and the moving mass, then the back-emf voltage is $v(t) = K_t\dot{x}(t)$. Thus, we have that the dynamics of harvester satisfy

$$m\ddot{x}(t) + c\dot{x}(t) + kx(t) = K_t i(t) + ma(t) \tag{1}$$

where $i(t)$ is the controllable transducer current and $a(t)$ is the disturbance acceleration. Through an appropriate change of coordinates (see [21]), the nondimensional harvester dynamics can be written in terms of the following self-dual state space

$$\dot{\mathbf{x}}_h(t) = \mathbf{A}_h\mathbf{x}_h(t) + \mathbf{B}_h i(t) + \mathbf{G}_h a(t) \tag{2a}$$
$$v(t) = \mathbf{B}_h^T\mathbf{x}_h(t) \tag{2b}$$

where

$$\mathbf{A}_h = \begin{bmatrix} 0 & 1 \\ -1 & -d \end{bmatrix}, \qquad \mathbf{B}_h = \begin{bmatrix} 0 \\ 1 \end{bmatrix}, \qquad \mathbf{G}_h = \begin{bmatrix} 0 \\ 1 \end{bmatrix}$$

and where $d = c/\sqrt{mk}$ is the damping ratio.

We assume the disturbance acceleration is filtered white noise. Specifically, we assume the disturbance can be modeled by a nondimensional first-order lowpass filter; i.e.,

$$\mathrm{d}x_a(t) = -\omega_c x_a(t)\mathrm{d}t + \sqrt{2\omega_c}\,\mathrm{d}w(t) \tag{3a}$$
$$a(t) = x_a(t) \tag{3b}$$

where $w(t)$ is a Weiner process normalized such that $\dot{w}(t)$ is white noise with unit spectral intensity, and ω_c is the nondimensional cutoff frequency of the lowpass filter. Note that the system is normalized such that $\mathcal{E}\{a^2\} = 1$ uniformly, as ω_c is varied. This allows us to compare accelerations of varying spectral content but equal intensity. Combining harvester and disturbance states such that $\mathbf{x}(t) = \begin{bmatrix}\mathbf{x}_h^T(t) & x_a(t)\end{bmatrix}^T$, results in the following state space realization

$$\mathrm{d}\mathbf{x}(t) = \{\mathbf{A}\mathbf{x}(t) + \mathbf{B}i(t)\}\,\mathrm{d}t + \mathbf{G}\mathrm{d}w(t) \tag{4a}$$
$$v(t) = \mathbf{B}^T\mathbf{x}(t) \tag{4b}$$

with appropriate definitions for $\mathbf{A}$, $\mathbf{B}$, and $\mathbf{G}$.

For this example, we consider a conservative approximation of the losses in the power electronics. Specifically, we define the energy harvesting performance measure as

$$\bar{P}_{gen} = -\mathcal{E}\{iv + Ri^2 + V_d|i|\} \tag{5}$$

where R and V_d are resistive and diode losses, respectively. This loss model corresponds to a power electronic converter in Fig. 1, which consists of a bridge rectifier connected to a PWM-switched controllable DC/DC converter. We assume the bridge rectifier is implemented actively, by gating MOSFETs to mimic diodes. Parasitic losses in an active rectifier are minimal because the MOSFETs only need to be gated when the direction of the current changes. The advantage of an active rectifier is that its conductive dissipation is quadratic in current, thus resembling a resistor. This is in contrast to a passive diode rectifier, which has a finite conduction voltage threshold. Because of this difference, even though active rectifiers require gating, their overall efficiency can be higher when the transducer current is very low.

Several studies [22]–[24] have demonstrated that operating a DC/DC converter in discontinuous conduction mode (DCM) results in a relationship between $i(t)$ and $v(t)$ that resembles a static admittance; i.e., $i(t) = -Y_s v(t)$. Those studies showed that the value of Y_s is proportional to the duty cycle of the converter. It would be straightforward to design a similar converter to the ones presented in those studies that realizes a time-varying admittance $Y(t)$. The single-directionality of DC/DC converters restricts the flow of power to extraction; i.e., $i(t)v(t) \leqslant 0,\ \forall t$. Furthermore, an additional constraint must be placed on the circuit such that the operating regime of the DC/DC converter is limited to DCM. Both of these conditions can be enforced by constraining $Y(t) \in [0, Y^{max}]$ where Y^{max} corresponds to the duty at which the converter transitions from the discontinuous to continuous conduction mode. These two restrictions result in the following power-flow constraint

$$i(t)v(t) + i^2(t)/Y^{max} \leqslant 0 \quad , \quad \forall t \, . \tag{6}$$

For the example in this paper, we assume that $Y^{max} = 1/R$.

With the modeling assumptions above, we can state a specific problem to solve:

$$\left.\begin{array}{lll} \text{Maximize} & : & \bar{P}_{gen} \\ \text{Over} & : & \phi : \mathbf{x}(t) \rightarrow i(t) \\ \text{Domain} & : & \{\phi(\cdot,\cdot) : \text{(6) holds}\} \end{array}\right\} \tag{7}$$

We next discuss the solution to energy harvesting problems such as this, via Hamilton-Jacobi theory.

III. Numerical Solution to the HJE via the Pseudospectral Method

A. Hamilton-Jacobi Theory

We begin by briefly recalling the standard stochastic Hamilton-Jacobi theory for constrained control systems. Consider the following generic single-input stochastic differential equation of the form

$$\mathrm{d}\mathbf{x}(t) = \{\mathbf{f}(\mathbf{x},t) + \mathbf{g}(\mathbf{x},t)u(t)\}\mathrm{d}t + \mathbf{h}(\mathbf{x},t)\mathrm{d}w(t) \tag{8}$$

where $u(t)$ is a generic control input (assumed to be scalar for brevity of exposition), while $w(t)$ and $\mathbf{x}(t)$ are the Wiener process and system state, respectively, as previously defined. If $\mathbf{f}(\mathbf{x},t)$ is linear, and $\mathbf{g}(\mathbf{x},t)$ and $\mathbf{h}(\mathbf{x},t)$ are constant, then (8) is also linear.

The generalized cost functional is

$$J = \mathcal{E}\left\{\int_0^\infty e^{-\beta\tau}\mathcal{L}(\mathbf{x},u,\tau)\ \mathrm{d}\tau\right\} < \infty \tag{9}$$

where $\mathcal{L}(\mathbf{x},u,t)$ is the Lagrangian, and $\beta > 0$ is an exponential discount factor. The value of β should be strictly greater than zero such that J is finite. However, it should be sufficiently small such that the initial condition of $\mathbf{x}(t)$ has a negligible impact on the value of J. In other words, the value of β is small enough such that $\mathcal{L}(\mathbf{x},u,t)$ reaches stationarity much faster than the exponential decay terms.

The objective is to solve for $\phi : \mathbf{x}(t) \rightarrow u(t)$ to minimize J subject to the constraint in (8). The standard necessary condition for optimality can be written in terms of the stochastic HJE. We first define the value (i.e., cost-to-go) function as

$$V(\mathbf{x},t) = \min_{\phi(\cdot,\cdot)}\left[\mathcal{E}\left\{\int_t^\infty e^{-\beta\tau}\mathcal{L}(\mathbf{x},\phi(\cdot,\cdot),\tau)\ \mathrm{d}\tau\right\}\right] \, . \tag{10}$$

Because the cost functional is defined on the infinite-time horizon, the resulting stationary solution for $V(\mathbf{x},t)$ will be time invariant. We denote the stationary optimal solution as $V^\star(\mathbf{x})$. From the stochastic optimality principle [25], [26], the stationary HJE can be expressed as

$$\begin{aligned}\beta V^\star(\mathbf{x}) = \min_u \Big[& V_{\mathbf{x}}^{\star T}\big(\mathbf{f}(\mathbf{x}) + \mathbf{g}(\mathbf{x})u\big) + \mathcal{L}(\mathbf{x},u) \\ & + \frac{1}{2}\mathrm{tr}\Big\{\mathbf{h}(\mathbf{x})\mathbf{h}^T(\mathbf{x})V_{\mathbf{xx}}^\star\Big\}\Big]\end{aligned} \tag{11}$$

where $V_{\mathbf{x}}^\star$ and $V_{\mathbf{xx}}^\star$ are the first and second partial derivatives of $V^\star(\mathbf{x})$ with respect to $\mathbf{x}$.

The optimal feedback control law $\phi^\star(\cdot)$ depends on the choice of the Lagrangian. For the purposes of this paper, the Lagrangian is a more specific version of the form

$$\mathcal{L}(\mathbf{x},u) = 2\mathbf{x}^T\mathbf{S}u + r(u) \tag{12}$$

where $r(\cdot)$ is positive-definite, continuous, and convex. We thus have that the optimal feedback law is

$$\phi^\star(\mathbf{x}) = \Phi\left(\mathbf{x}, V_{\mathbf{x}}^\star\right) \tag{13}$$

where

$$\Phi(\mathbf{x}, V_{\mathbf{x}}^\star) = \arg\min_u \left\{(\mathbf{g}^T(\mathbf{x})V_{\mathbf{x}} + 2\mathbf{S}^T\mathbf{x})u + r(u)\right\} \, . \tag{14}$$

The optimal feedback law has a unique solution for the assumptions made above for $r(\cdot)$, and is continuous in both arguments assuming $\mathbf{g}(\mathbf{x})$ is itself continuous. Substituting (13) into (11) gives the partial differential equation to be solved over $\mathbf{x}$, as

$$\begin{aligned}\beta V^\star(\mathbf{x}) = {} & V_{\mathbf{x}}^{\star T}\mathbf{f}(\mathbf{x}) + (\mathbf{g}^T(\mathbf{x})V_{\mathbf{x}}^\star + 2\mathbf{S}^T\mathbf{x})\Phi(\mathbf{x}, V_{\mathbf{x}}^\star) \\ & + r(\Phi(\mathbf{x}, V_{\mathbf{x}}^\star)) + \frac{1}{2}\mathrm{tr}\Big\{\mathbf{h}(\mathbf{x})\mathbf{h}^T(\mathbf{x})V_{\mathbf{xx}}^\star\Big\} \, .\end{aligned} \tag{15}$$

Equation (15) is the stationary HJE that must be solved to obtain the optimal value function $V^\star(\mathbf{x})$. Once the optimal value function has been determined, the optimal controller $u^\star(\mathbf{x})$ can be obtained using (13).

If $r(u)$ is quadratic; i.e., $r(u) = Ru^2$, and if the system in (8) is linear, then the resulting HJE can be reduced to the standard algebraic Riccati equation. Scruggs showed in [8] that the solution to this resultant Riccati equation is asymptotically stabilizing, assuming the forward loop transfer function is positive real in the weakly-strict sense. It turns out that this caveat is still enough to guarantee asymptotic closed-loop stability for optimal feedback law $\phi^\star(\cdot)$ when $r(u)$ is nonquadratic, so long as it satisfies the assumptions we have made above. (In this interest of brevity this result is not proven here.) However, in the more general case of nonquadratic $r(u)$, there is no closed form solution to (15) even if (8) is linear.

There are a number of technical challenges associated with solving the HJE, which is a second order nonlinear partial differential equation. Numerical grid-based techniques such as finite element or finite difference methods suffer from the "curse-of-dimensionality," which refers to the exponential scaling of computational effort required to solve problems with linearly increasing dimensions. We therefore implement the combined successive approximation and pseudospectral method proposed by Song and Dyke [20] to solve the HJE.

B. The Pseudospectral Method

We now introduce the pseudospectral (PS) method, which will be used in conjunction with the successive approximation method to solve the stationary HJE in (11). The PS method is a numerical technique that can be used to approximate the solution to a partial differential equation over an entire computational domain. Compared to the polynomial decay rate of similar finite element and finite difference methods, the approximation error of the PS method decays at an exponential rate. As a consequence of the higher accuracy of the PS method, the required number of grid points and subsequent number of degrees of freedom can be minimized to reduce the computational effort.

To simplify the math, we describe the PS method in detail for a one-dimensional state space. Then, the natural extension to multiple dimensions is briefly explained. The PS method used in this paper is based on interpolation functions collocated on Chebyshev nodes, which are distributed over the interval $\xi \in [-1, 1]$. To accommodate the use of an arbitrary computation domain $x \in [x_0, x_f]$, we use the following affine transformation

$$x(\xi) = \frac{(x_f - x_0)\xi + (x_f + x_0)}{2} \quad , \quad \xi \in [-1, 1] \tag{16}$$

where we define the slope constant as

$$m = \frac{\mathrm{d}x}{\mathrm{d}\xi} = \frac{x_f - x_0}{2} \ . \tag{17}$$

The solution to the HJE can be approximated by a truncated polynomial $V_{N-1}(x)$ of order $N-1$ with N interpolation nodes. For the single-dimensional case, this approximation can be expressed as

$$V_{N-1}(x) = \sum_{i=1}^{N} v_i \psi_i(x) \tag{18}$$

where $\psi_i(x)$ is a set of polynomial basis functions and v_i is the corresponding interpolation coefficient. In this paper, Lagrange polynomial interpolation functions are used and the interpolation nodes are chosen at Chebyshev nodes; i.e.,

$$\xi_k = \cos\left(\frac{k\pi}{N}\right) \quad , \quad k = 1..N \ . \tag{19}$$

Using the Lagrange polynomial functions and the Chebyshev nodes, we can approximate partial derivative of (18) at node x_i for $i \in [1, N]$ as

$$V_{N-1}^{(\ell)}(x_i) = \sum_{j=1}^{N} \mathbf{D}_{i,j}^{(\ell)} v_j \quad , \quad i = 1..N \tag{20}$$

where the superscript $(\cdot)$ indicates the order of the derivative and where $\mathbf{D}_{i,j}^{(\ell)}$ is the differentiation matrix defined on $[x_0, x_f]$. The differentiation matrix is derived, for example, in [13]. Equation (20) can be written in vector form as

$$\mathbf{V}_{N-1}^{(\ell)} = \mathbf{D}^{(\ell)}\mathbf{v} = \left(\mathbf{D}^{(1)}\right)^{\ell}\mathbf{v} \tag{21}$$

where $\mathbf{V}_{N-1}^{(\ell)}$ and $\mathbf{v}$ are the column vector forms of $V_{N-1}^{(\ell)}(x_i)$ and v_i, respectively.

Using the vector relationship for the value function in (21), we can discretize the original HJE in (15) over the computational domain $x \in [x_0, x_f]$. The discretized HJE at the i-th Chebyshev node x_i can be written as

$$\begin{aligned} &\Big(\mathbf{f}^T\mathbf{D}_i + \left(\Phi(\mathbf{x}_i, \mathbf{D}_i\mathbf{v}_i)\right)^T \mathbf{g}^T\mathbf{D}_i - \beta\mathbf{I}_i\Big)\mathbf{v}_i \\ &+\frac{1}{2}\mathrm{tr}\Big\{\mathbf{h}\mathbf{h}^T\mathbf{D}_i^{(2)}\mathbf{v}_i\Big\} = -\mathcal{L}(\mathbf{x}_i, \Phi(\mathbf{x}_i, \mathbf{D}_i\mathbf{v}_i)) \end{aligned} \tag{22}$$

where the subscript i indicates the i-th row of the corresponding matrix. Setting up similar discretized equations for the remaining Chebyshev nodes results in a system of N equations where the unknowns to be solved are the N values of the vector $\mathbf{v}$.

C. Iterative Algorithm

Because of the challenges associated with explicitly solving (22), we combine the PS method with the successive approximation algorithm to solve the discretized HJE.

Step 0 : Start with an initial stabilizing truncated controller $\phi_{N-1}^0(x)$, which can be found as

$$\phi_{N-1}^0(\mathbf{x}_i) = \sum_{i=1}^{N} \phi_i^0 \psi_i(x) \tag{23}$$

where ϕ_i is the nodal value of the chosen initial control law at the i-th Chebyshev node. For this paper, we assume that ϕ^0 is the optimal controller of the corresponding linear system.

Step 1 : Given ϕ^0, set up N linear equations for $i \in [1, N]$ of the form

$$\begin{aligned} &\Big(\mathbf{f}^T\mathbf{D}_i + (\phi_i^0)^T\mathbf{g}^T\mathbf{D}_i - \beta\mathbf{I}_i\Big)\mathbf{v}_i \\ &+\frac{1}{2}\mathrm{tr}\Big\{\mathbf{h}\mathbf{h}^T\mathbf{D}_i^{(2)}\mathbf{v}_i\Big\} = -\mathcal{L}(\mathbf{x}_i, \phi_i^0) \end{aligned} \tag{24}$$

where $\mathbf{D}_i$ and $\mathbf{I}_i$ are the i-th rows of $\mathbf{D}$ and $\mathbf{I}$, respectively. The resulting system of equations is linear in $\mathbf{v}$, and thus its solution is immediate.

Step 2 : Update the discretized controller on each of the i nodes as $\phi_i^0 \leftarrow \Phi(\mathbf{x}_i, \mathbf{D}_i\mathbf{v})$ and return to Step 1.

Convergence of the combined PS and successive approximation algorithm is discussed in [20].

It is straightforward to extend the combined PS and successive approximation algorithm for systems with multiple dimensions. The main difference between the single- and multi-dimensional cases is in the derivation of the multi-dimensional differentiation matrix. Instead of expressing the truncated polynomial V_{N-1} as a tensor product, the analysis can be simplified by combining the grid points for each dimension into a single vector. As such, the multi-dimensional differentiation matrix can be assembled using components of the single-dimensional differentiation matrices for each node in each dimension [20].

IV. Application to the Energy Harvesting Problem

For the energy harvesting problem at hand, the control input is the transducer current; i.e., $u(t) = i(t)$, and the Lagrangian is the negative of generated power; i.e.,

$$\mathcal{L}(\mathbf{x}, i, t) = i(t)\mathbf{B}^T\mathbf{x}(t) + Ri^2(t) + V_d|i(t)| \,. \tag{25}$$

The corresponding optimal PS performance can be expressed as

$$\bar{P}_{gen}^{PS} = -\lim_{T\to\infty} \mathcal{E}\left\{\frac{1}{T}\int_0^T \mathcal{L}(\mathbf{x}, \phi^\star(\mathbf{x}), \tau)\ \mathrm{d}\tau\right\} \tag{26}$$

which is equivalent to

$$\bar{P}_{gen}^{PS} = -\lim_{\beta\to 0}\ \beta V^\star(\mathbf{0}) \,. \tag{27}$$

In the example to be discussed shortly, β is finite but made sufficiently small relative to the open-loop dynamics of $\mathbf{A}$ (i.e., $\beta < \frac{1}{100}\min_i |\mathbb{R}(\lambda_i(\mathbf{A}))|$), such that the limit above is nearly reached.

By application of the results from Section III-A, it is straightforward to verify that

$$\Phi(\mathbf{x}, V_\mathbf{x}) = -\underset{[0,Y^{max}]}{\mathrm{sat}}\left\{\frac{-\Phi_u(\mathbf{x}, V_\mathbf{x})}{\mathbf{B}^T\mathbf{x}}\right\}\mathbf{B}^T\mathbf{x} \tag{28}$$

where $\Phi_u(\mathbf{x}, V_\mathbf{x})$ is the unconstrained controller; i.e.,

$$\Phi_u(\mathbf{x}, V_\mathbf{x}) = \begin{cases} -\frac{1}{2R}\theta & : \ \theta < 0 \\ -\frac{1}{2R}\theta & : \ \theta > 0 \\ 0 & : \ \text{otherwise} \end{cases} \tag{29}$$

and where $\theta = \mathbf{B}^T\left(V_\mathbf{x}+\mathbf{x}\right)+V_d$. Thus, the optimal controller is

$$\phi^\star(\mathbf{x}) = -\underset{[0,Y^{max}]}{\mathrm{sat}}\left\{\frac{-\Phi_u(\mathbf{x}, V_\mathbf{x}^\star)}{\mathbf{B}^T\mathbf{x}}\right\}\mathbf{B}^T\mathbf{x} \,. \tag{30}$$

Note that this is equivalent to an optimal state-dependent electronic input admittance $Y^\star(\mathbf{x})$ equal to

$$Y^\star(\mathbf{x}) = \underset{[0,Y^{max}]}{\mathrm{sat}}\left\{\frac{-\Phi_u(\mathbf{x}, V_\mathbf{x}^\star)}{\mathbf{B}^T\mathbf{x}}\right\} \,. \tag{31}$$

A. Results

We compare the performance of the PS controller to the performance of the optimal static admittance (SA) controller; i.e., $i(t) = -Y_s v(t)$, where $Y_s \in [0, Y^{max}]$. For reference, we also compute the performance of the unconstrained optimal full-state LQG controller; i.e., $i(t) = \mathbf{K}\mathbf{x}(t)$, where $\mathbf{K}$ is the LQG feedback gain. The diode losses are accounted for in the design of the SA and LQG controllers using the procedure discussed in [27]. To illustrate the improvement in performance achieved by the PS controller, we plot the performance ratios $\bar{P}_{gen}^{SA}/\bar{P}_{gen}^{PS}$ and $\bar{P}_{gen}^{PS}/\bar{P}_{gen}^{LQG}$ over a range of $\{\omega_c, R\}$ values and for three increasing values of V_d. We note that the PS algorithm is unable to converge to a solution when ω_c and R approach 0. Therefore, those parameters were limited to be within the range $[0.1, 10]$.

First, we consider the case in which we have purely quadratic losses (i.e., $V_d = 0$). The plots in Figs. 2(a) and 2(b) illustrate the performance ratios for $V_d = 0$. From the plot in Fig. 2(a), the SA and PS performances are almost identical except when ω_c is near unity and $R \to 0$. Furthermore, Fig. 2(b) clearly shows that the unconstrained LQG controller significantly outperforms the PS controller for all values of ω_c and R.

Next, we modify our example to include two nonzero values for the diode losses. The plots in Figs. 2(c) and 2(d) show the performance ratios for the case where $V_d = 0.2$ while the plots in Fig. 2(e) and 2(f) show the performance ratios for the case where $V_d = 0.4$. From these two cases, we obtain the interesting result that there are regions in the $\{\omega_c, R\}$ space in which the PS controller outperforms the unconstrained LQG controller. This is because the unconstrained LQG controller is restricted to linear feedback, which is only proven to be optimal when diode losses are zero, whereas the PS controller is nonlinear in the system states. As V_d increases, much more power is generated by the PS controller as compared to the unconstrained LQG controller for values of ω_c away from unity. However, as shown in Fig. 2(d), the unconstrained LQG slightly outperforms the PS controller for values of ω_c near unity and as $R \to 0$.

V. Conclusions

The purpose of this paper has been to compute optimal numerical feedback controllers for energy harvesters with power-flow constraints. Determining controllers for constrained systems requires a solution to the stochastic HJE, which is challenging because it is a nonlinear partial differential equation. Thus, we present an iterative approach to compute the discretized control manifold using the combined PS and successive approximation algorithm from [20]. However, unlike the examples considered in that paper, we explored the ability of the algorithm to handle a mixed state-control constraint. The performance of the PS controller was compared to the performances of the optimal SA controller and the unconstrained LQG controller for a SDOF energy harvester with electromagnetic coupling. From this example, we found that the PS controller outperforms the unconstrained LQG controller for certain $\{\omega_c, R\}$ regions when $V_d > 0$. For higher values of V_d, the PS controller always outperforms the unconstrained LQG controller over the entire $\{\omega_c, R\}$ domain.

However, there are two drawbacks to the PS control approach. The first drawback relates to the synthesis of the control input from the discretized control manifold. Because the discretized control manifold is a function of the grid nodes, an approximate value of the control input could be computed from a polynomial expansion of the states at each node. This approach is very computationally demanding, especially for grids with higher resolution, and it may not be feasible to implement a control algorithm

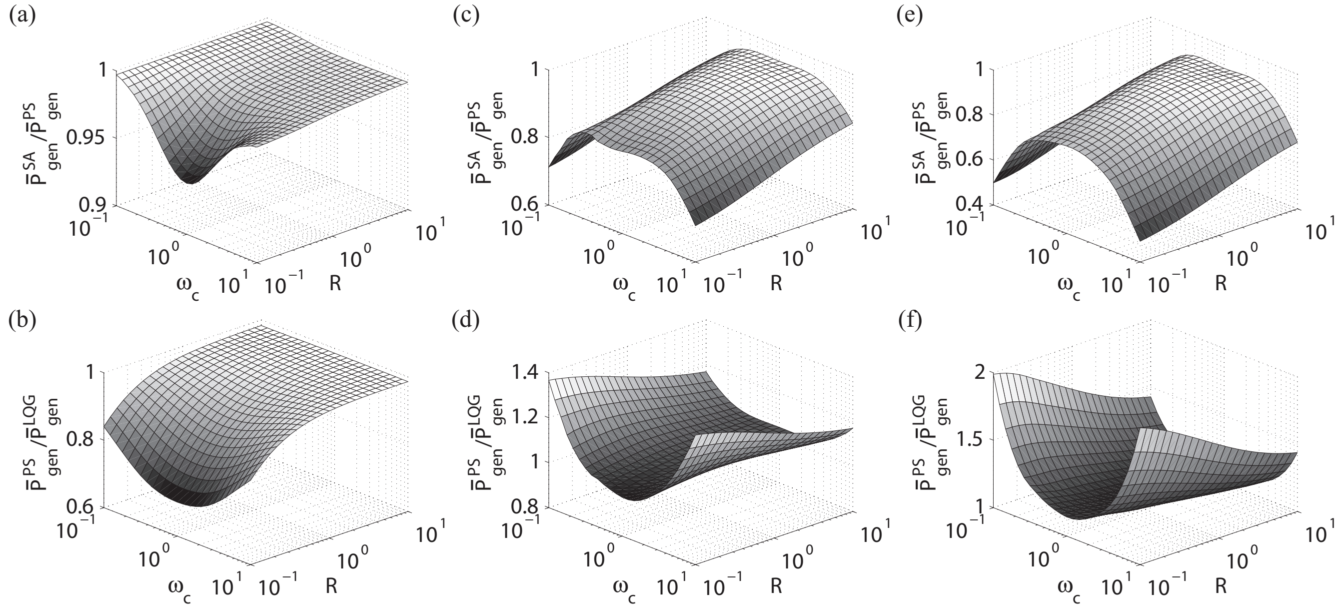

Fig. 2. Performance ratios as a function of $\{\omega_c, R\}$ for $d = 0.1$: (a) $\bar{P}^{SA}_{gen}/\bar{P}^{PS}_{gen}$ for $V_d = 0$, (b) $\bar{P}^{PS}_{gen}/\bar{P}^{LQG}_{gen}$ for $V_d = 0$, (c) $\bar{P}^{SA}_{gen}/\bar{P}^{PS}_{gen}$ for $V_d = 0.2$, (d) $\bar{P}^{PS}_{gen}/\bar{P}^{LQG}_{gen}$ for $V_d = 0.2$, (e) $\bar{P}^{SA}_{gen}/\bar{P}^{PS}_{gen}$ for $V_d = 0.4$, and (f) $\bar{P}^{PS}_{gen}/\bar{P}^{LQG}_{gen}$ for $V_d = 0.4$.

of this type in a physical system in real time. Second, because of the limitation on computational power required for the PS algorithm to converge, the computational domain must be made increasingly coarse as the number of states increases, which results in a less accurate controller. Thus, the PS control approach may not be suitable for systems with multiple modes (e.g., piezoelectric energy harvesters).

REFERENCES

[1] S. Roundy, P. K. Wright, and J. Rabaey, "A study of low level vibrations as a power source for wireless sensor nodes," *Journal of Computer Communications*, vol. 26, pp. 1131–1144, 2002.

[2] R. Amirtharajah and A. P. Chandrakasan, "Self-powered signal processing using vibration-based power generation," *IEEE Journal of Solid-State Circuits*, vol. 33, pp. 687–695, 1998.

[3] S. R. Anton and H. A. Sodano, "A review of power harvesting using piezoelectric materials (2003-2006)," *Smart Materials and Structures*, vol. 16, pp. R1–R21, 2007.

[4] S. P. Beeby, M. J. Tudor, and N. M. White, "Energy harvesting vibration sources for microsystems applications," *Measurement Science and Technology*, vol. 17, pp. R175–R195, 2006.

[5] J. A. Paradiso and T. Starner, "Energy scavenging for mobile and wireless electronics," *Pervasive Computing*, pp. 18–27, January-March 2005.

[6] S. Priya and D. J. Inman, *Energy Harvesting Technologies*, Springer, 2009.

[7] J. T. Scruggs, "An optimal stochastic control theory for distributed energy harvesting networks," *Journal of Sound and Vibration*, vol. 320, pp. 707–725, 2009.

[8] J. T. Scruggs, "On the causal power generation limit for a vibratory energy harvester in broadband stochastic response," *Journal of Intelligent Material Systems and Structures*, vol. 21, pp. 1249–1262, 2010.

[9] J. T. Scruggs, I. L. Cassidy, and S. Behrens, "Multi-objective optimal control of vibratory energy harvesting systems," *Journal of Intelligent Material Systems & Structures*, vol. 23, pp. 2077–2093, 2012.

[10] M. Boulbrachene and M. Haiour, "The finite element approximation of hamilton-jacobi-bellman equations," *Computers and Mathematics with Applications*, vol. 41, pp. 993–1007, 2001.

[11] S. Wang, L. S. Jennings, and K. L. Teo, "Numerical solution of hamilton-jacobi-bellman equations by an upwind finite volume method," *Journal of Global Optimization*, vol. 27, pp. 177–192, 2003.

[12] J. P. Boyd, *Chebyshev and Fourier Spectral Methods (2nd ed.)*, Dover, 2000.

[13] C. Canuto, M. Y. Hussaini, A. Quarteroni, and T. A. Zang, *Spectral Methods in Fluid Dynamics*, Springer-Verlag, 1998.

[14] B. Fronberg, *A Practical Guide to Pseudospectral Methods*, Cambridge University Press, 1995.

[15] G. Elnager and M. A. Kazemi, "Pseudospectral chebyshev optimal control of constrained nonlinear dynamical systems," *Computational Optimization and Applications*, vol. 11, pp. 195–217, 1998.

[16] G. Elnager, M. A. Kazemi, and M. Razzaghi, "The pseudospectral legendre method for discretizing optimal control problems," *IEEE Transactions on Automatic Control*, vol. 40, pp. 1793–1796, 1995.

[17] F. Fahroo and I. M. Ross, "Pseudospectral methods for infinite-horizon optimal control problems," *Journal of Guidance, Control, and Dynamics*, vol. 24, pp. 927–936, 2008.

[18] Q. Gong, W. Kang, and I. M. Ross, "A pseudospectral method for the optimal control of constrained feedback linearizable systems," *IEEE Transactions on Automatic Control*, vol. 51, pp. 1115–1129, 2006.

[19] W. Song and S. J. Dyke, "A general numerical solution to optimal nonlinear stochastic structural control problem," in *Proc. of SPIE Vol. 7647*, 2010.

[20] W. Song and S. J. Dyke, "Optimal feedback design for nonlinear stochastic systems using the pseudospectral method," *International Journal of Non-Linear Mechanics*, 2012, Under Review.

[21] I. L. Cassidy, J. T. Scruggs, and S. Behrens, "Optimization of partial-state feedback for vibratory energy harvesters subjected to broadband stochastic disturbances," *Smart Materials and Structures*, vol. 20, 2011, #085019.

[22] N. Kong, D. S. Ha, A. Erturk, and D. J. Inman, "Resistive impedance matching circuit for piezoelectric energy harvesting," *Journal of Intelligent Material Systems and Structures*, vol. 21, pp. 1293–1302, 2010.

[23] G. K. Ottman, H. F. Hofmann, and G. A. Lesieutre, "Optimized piezoelectric energy harvesting circuit using step-down converter in discontinuous conduction mode," *IEEE Transactions On Power Electronics*, vol. 18, pp. 696–703, 2003.

[24] T Paing, J. Shin, R. Zane, and Z. Popovic, "Resistor emulation approach to low-power rf energy harvesting," *IEEE Transactions on Power Electronics*, vol. 23, pp. 1494–1501, 2008.

[25] P. Dorato, C. T. Abdallah, and V. Cerone, *Linear-Quadratic Control: An Introduction*, Prentice Hall, 1995.

[26] W. H. Fleming and H. M. Soner, *Controlled Markov Processes and Viscosity Solutions*, Springer, 2006.

[27] I. L. Cassidy and J. T. Scruggs, "Statistically linearized optimal control of an electromagnetic vibratory energy harvester," *Smart Materials and Structures*, vol. 20, 2012, #085003.